Secondary gamma rays from ultrahigh energy cosmic rays produced in magnetized environments

Eric Armengaud,[1,2] Günter Sigl,[1,2] and Francesco Miniati[3]

[1]*APC (AstroParticules et Cosmologie), 11, place Marcelin Berthelot, F-75005 Paris, France**

[2]*GReCO, Institut d'Astrophysique de Paris, C.N.R.S., 98 bis boulevard Arago, F-75014 Paris, France*

[3]*Physics Department, ETH Zürich, 8093 Zürich, Switzerland*

(Received 9 November 2005; revised manuscript received 3 February 2006; published 24 April 2006)

Nearby sources of cosmic rays up to a ZeV($= 10^{21}$ eV) could be observed with a multimessenger approach including secondary γ-rays and neutrinos. If cosmic rays above $\sim 10^{18}$ eV are produced in magnetized environments such as galaxy clusters, the flux of secondary γ-rays can be enhanced by a factor ~ 10 at Gev energies and by a factor of a few at TeV energies, compared to unmagnetized sources. Particularly enhanced are synchrotron and cascade photons from e^+e^- pairs produced by protons from sources with relatively steep injection spectra $\propto E^{-2.6}$. Such sources should be visible at the same time in ultrahigh energy cosmic ray experiments and γ-ray telescopes.

DOI: 10.1103/PhysRevD.73.083008 PACS numbers: 98.70.Sa, 98.65.Cw, 98.70.Rz

I. INTRODUCTION

One of the central unresolved issues of modern astroparticle physics is the origin of cosmic rays, particularly those at Ultra High Energy (UHECR) which have been observed at energies up to a few times 10^{20} eV [1]. Sources capable of accelerating such particles, like powerful radio galaxies commonly found inside galaxy clusters and groups, are thought to be rare [2] and have yet to be identified.

Astroparticle physics is currently experimentally driven and involves many different existing or planned projects ranging from UHECR observatories such as the Pierre Auger project [3], to neutrino telescopes [4], as well as ground and space based γ-ray detectors operating at TeV and GeV energies, respectively [5]. It is clear that GeV-TeV γ-ray and neutrino astronomy will prove an invaluable tool to unveil the sources, and probe into the mechanism, of UHECRs. Even if a putative source were to produce exclusively UHECRs, photo-pion [6] and pair production by protons on the cosmic microwave background (CMB) would lead to a guaranteed secondary photon and neutrino fluxes that could be detectable.

Secondary photon fluxes from UHECR interactions with the CMB have been discussed before in the literature: In Ref. [7] rather weak, extended fields of order nano Gauss have been considered, in Ref. [8] magnetic fields have been neglected, and in Ref. [9] magnetic fields in galaxy clusters have been considered, but only analytical estimates of secondary γ-ray fluxes have been performed. A semianalytical treatment of photon production by cosmic rays in galaxy clusters has been given in Ref. [10]. In Ref. [11] proton acceleration up to $\sim 10^{19}$ eV around cluster accretion shocks was studied which, however, can not explain the highest energy cosmic rays.

In the present work we study numerically the effects of structured magnetic fields of order μG, as they occur in galaxy clusters, on the production of secondary photon fluxes from sources of UHECRs. Magnetic fields affect nonlinearly both the propagation of UHECRs and the electromagnetic (EM) cascade initiated by the latter through photo-pair and pion production. Our results indicate that secondary photon fluxes from individual UHECR sources can be substantially enhanced, up to a factor of a few at TeV energies and an order of magnitude around GeV energies. This potentially makes their detection much easier.

Furthermore, we extend the investigation to also consider the case of steep proton spectra $\propto E^{-2.6}$ at ultrahigh energies. This is motivated by the scenario where extragalactic protons dominate the observed flux down to the "second knee" at $\simeq 4 \times 10^{17}$ eV, such that the ankle at $\simeq 5 \times 10^{18}$ eV is caused by photo-pair production by the extragalactic protons [12,13].

In Sec. II we describe the simulations, Sec. III discusses the influence of pair production and proton injection spectra on the GeV-TeV photon flux, and Sec. IV considers the magnetized scenario. Conclusions can be found in Sec. V. We use $c = 1$ throughout the paper.

II. SIMULATIONS

In the following we compute the expected γ-ray flux from ~ 10 MeV to the highest energies, due to the processes described in the Introduction section. We combine 3 dimensional simulations of UHECR propagation in structured large scale extragalactic magnetic fields [14] (EGMF) with the simulation of EM cascades generated by these UHECRs. Photo-pion production on the CMB is handled by the event generator SOPHIA [15]. Pair production by protons on the CMB, also known as Bethe-Heitler process, is taken into account as a continuous energy loss whose rate we evaluate following the expressions in Refs. [16,17]. Our code integrates trajectories in small

*UMR 7164 (CNRS, Université Paris 7, CEA, Observatoire de Paris)

steps over each of which the total energy loss to pair production is integrated. This assures that the correct fraction of proton energy is lost to pair production which is typically smaller than 10^{-3} Mpc^{-1}. For the spectrum of the pairs we exploit the fact that Bethe-Heitler and triplet pair production, $e\gamma_b \rightarrow ee^+e^-$, are analogous electromagnetic processes with very similar quantum mechanical transition amplitudes. As a result, their differential and total cross sections and inelasticities become very similar for relativistic pairs. Fig. 2 of Ref. [18] then shows that the spectrum of electron-positron pairs (heretoafter simply referred to as electrons) generated by a proton of energy E can be approximated by a power-law energy distribution $dn/dE_e \propto E_e^{-7/4}$. Kinematics implies that this power law extends up to [19]

$$E_{\rm PPP} \simeq \frac{4E^2\varepsilon}{4E\varepsilon + m_p^2} \sim \frac{4.5\times 10^{15}(\frac{E}{\rm EeV})^2}{4.6\times 10^{-3}(\frac{E}{\rm EeV})+1}\ {\rm eV}, \quad (1)$$

where m_p is the proton mass and for the typical CMB photon energy we have inserted $\varepsilon \simeq 10^{-3}$ eV in the numerical estimate.

All the electromagnetic products of these interactions are then followed to the observer using an EM cascade code based on Ref. [19], which takes into account the inhomogeneous distribution of magnetic fields in the simulation box and the presence of a cosmic infrared background from [20].

While the full trajectories of protons are followed down to 10^{18} eV, the EM cascades are simulated by solving one-dimensional transport equations. This is a good approximation in all relevant regimes of our simulations: In the interior of galaxy clusters for fields of strength $B \gtrsim 0.1\ \mu$G electrons with energies $E_e \gtrsim 3\times 10^{17}$ eV loose energy by synchrotron radiation before being deflected significantly. For $E_e \gtrsim 10^{15}$ eV and $B \lesssim 1$ nG and for $E_e \gtrsim 1$ TeV and $B \lesssim 10^{-12}$ G electrons undergo inverse Compton scattering before being significantly deflected. Electrons at lower energies, where the one-dimensional EM cascade approximation would break down, do not significantly contribute to γ-ray fluxes above 10 MeV, which we are interested in.

In the following, we assume UHECR point sources whose flux contributes a fraction $\eta \leq 1$ to the total solid angle integrated UHECR flux observed around 10^{19} eV, i.e. $\simeq 2.5\times 10^{-19}(\eta/0.01)$ cm^{-2} s^{-1}, the approximate average over existing flux measurements [1]. For distances $d \lesssim 500$ Mpc this flux is not too much influenced by energy losses and roughly correponds to an UHECR injection power above 10^{19} eV of

$$L_{19} \simeq 4.8\times 10^{42}\left(\frac{d}{100\ {\rm Mpc}}\right)^2\left(\frac{\eta}{0.01}\right)\ {\rm erg\,s^{-1}}. \quad (2)$$

III. INFLUENCE OF PAIR PRODUCTION AND PROTON INJECTION SPECTRA ON GEV-TEV PHOTON FLUXES

Figure 1 compares the contributions of pair production and pion production to the secondary γ-ray fluxes. At GeV and TeV energies, the importance of pair production increases with the steepness of the proton injection spectrum because pair production is the dominant energy loss process for protons with energies $10^{18} \lesssim E \lesssim 4\times 10^{19}$ eV. It appears that, for steep enough injection spectrum $\propto E^{-\alpha}$ with $\alpha \sim 2.6$–2.7, necessary if extragalactic cosmic rays dominate above the ankle [12,13], and sufficiently large distances between the source and the observer, photo-pair production dominates over pion production for the secondary γ-ray flux. In general, however, pion production and pair production lead to γ-ray fluxes of the same order of magnitude, and both must therefore be taken into account.

Above $\sim 10^{16}$ eV, photon fluxes are higher for harder proton injection spectra (smaller α). In addition, above 10^{18} eV the flux is dominated by pion production whereas between 10^{14} and 10^{18} eV it is dominated by pair production.

We now investigate the consequences of the low energy extension of the UHECR injection spectrum.

Cosmic ray protons of energy E and integral flux $J^{\rm l}_{\rm CR}(E)$ confined within a volume $\simeq R^3$ which interact with a baryon gas of density n_b produce γ-rays of energy $\simeq f_\gamma E \simeq 0.1E$ at a rate $\simeq J^{\rm l}_{\rm CR}(E)\sigma_{pp}n_bR^3$. Here, the proton-proton cross section $\sigma_{pp} \simeq 3\times 10^{-26}$ cm^2 can be

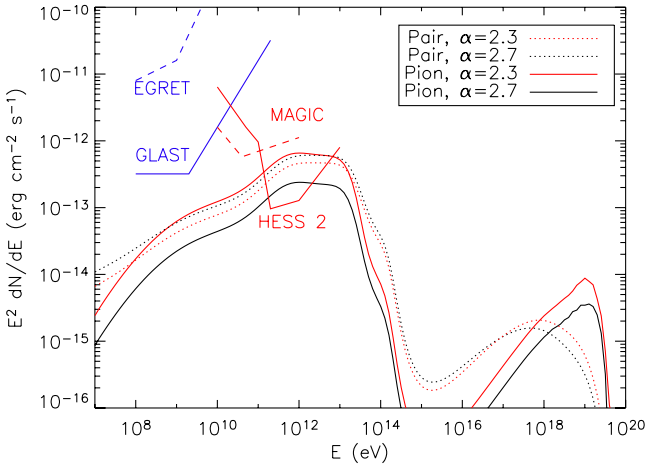

FIG. 1 (color online). Comparison of differential γ-ray fluxes (multiplied by squared energy) generated by GZK interactions and photo-pair production for a source at 100 Mpc distance injecting protons up to 1 ZeV with a spectrum $\propto E^{-2.7}$ (black lines) and with a spectrum $\propto E^{-2.3}$ (red lines) in the absence of magnetic fields. The power emitted above 10^{19} eV is $L_{19} = 10^{43}$ erg s^{-1}, contributing a fraction $\eta \simeq 0.02$ to the total UHECR flux, see Eq. (2). Also shown are point flux sensitivities of the γ-ray instruments EGRET [21], GLAST [26], HESS 2 [27], and MAGIC [28].

approximated as energy independent. For proton confinement times $t_{\rm conf}(E) \gtrsim R$, we can express the confined integral flux in terms of the total injection rate $I_{\rm CR}^{\rm inj}(E)$ as $J_{\rm CR}^{\rm l}(E) \simeq I_{\rm CR}^{\rm inj}(E) t_{\rm conf}(E)/R^3$. Furthermore, in a steady state situation, the leaking cosmic ray flux observed at a distance d is $J_{\rm CR}^{\rm obs}(E) \simeq M(E) I_{\rm CR}^{\rm inj}(E)/(4\pi d^2)$, where $M(E) \lesssim 1$ is a modification factor accounting for interaction losses during propagation to the observer. We can then relate the integral photon flux at energy above E_γ from pp interactions within the volume R^3, $J_\gamma^{pp}(E_\gamma)$, to the integral UHECR flux above $E_{\rm CR}$, $J_{\rm CR}^{\rm obs}(E_{\rm CR})$,

$$J_\gamma^{pp}(E_\gamma) \simeq \sigma_{pp} n_b t_{\rm conf}(E_\gamma/f_\gamma) \frac{I_{\rm CR}^{\rm inj}(E_\gamma/f_\gamma)}{I_{\rm CR}^{\rm inj}(E_{\rm CR})} \frac{J_{\rm CR}^{\rm obs}(E_{\rm CR})}{M(E_{\rm CR})}. \tag{3}$$

Both J_γ^{pp} and $J_{\rm CR}^{\rm obs}(E_{\rm CR})$ are fluxes observed at distance d.

For a galaxy cluster $n_b \sim 10^{-3}$ cm^{-3}, $R \simeq 2$ Mpc and $t_{\rm conf}(E_\gamma/f_\gamma) \lesssim 10^{10}$ yr (the age of the Universe). Thus, the optical depth for pp interaction is $\sigma_{pp} n_b t_{\rm conf} \lesssim 0.3$. Furthermore, at $E_{\rm CR} \simeq 10^{19}$ eV, $M(E_{\rm CR}) \simeq 1$ and with the cosmic ray flux from Eq. (2) we have

$$J_\gamma^{pp}(E_\gamma) \simeq 7.5 \times 10^{-20} \left(\frac{\eta}{0.01}\right) \frac{I_{\rm CR}^{\rm inj}(E_\gamma/f_\gamma)}{I_{\rm CR}^{\rm inj}(10^{19}\ {\rm eV})}\ {\rm cm}^{-2}\,{\rm s}^{-1}. \tag{4}$$

The upper limit on the γ-ray flux at $E_\gamma \sim 100$ MeV from EGRET is typically $\sim 4 \times 10^{-8}$ cm^{-2} s^{-1} for clusters like Coma or Virgo [21]. Equation (4) thus implies the condition

$$\frac{I_{\rm CR}^{\rm inj}(E_\gamma/f_\gamma \sim 10^9\ {\rm eV})}{I_{\rm CR}^{\rm inj}(10^{19}\ {\rm eV})} \lesssim 5.3 \times 10^{11} \left(\frac{0.01}{\eta}\right). \tag{5}$$

For an unbroken power law $I_{\rm CR}^{\rm inj}(E) \propto E^{1-\beta}$ with $E_\gamma/f_\gamma \sim 10^9$ eV $\lesssim E \lesssim 10^{19}$ eV, this would imply the relatively strong constraint

$$\beta \lesssim 2.17 - 0.1 \log_{10}(\eta/0.01). \tag{6}$$

This constraint can be avoided if the power law is broken such that it becomes harder at low energies and Eq. (5) is satisfied. In particular, in the scenario in which extragalactic protons dominate down to a few 10^{17} eV, their injection spectrum, $\alpha \simeq 2.6$ [12,13], cannot continue below $\sim 10^{11+\log(\eta/0.01)/1.6}$ eV.

At the same time, for $\beta \gtrsim 2.$, the total power emitted by the source in cosmic rays down to energy $E_{\rm CR}^{\rm min}$ is $L_{\rm CR} \simeq (10^{19}\ {\rm eV}/E_{\rm CR}^{\rm min})^{\beta-2} L_{19}$. Therefore, low energy cosmic ray flux extensions with power law index not much larger than 2 also assure reasonable total cosmic ray powers which remain largely below the high end of bolometric luminosity for AGNs, $L \lesssim 10^{48}$ erg s^{-1}.

IV. SOURCES IN MAGNETIZED GALAXY CLUSTERS

In this section we consider the case of a discrete source in one of the prominent magnetized galaxy clusters from the simulations based on Refs. [22,23], with a size comparable to the Virgo cluster. In the chosen configuration shown in Fig. 2, fields of 0.1–1 μG exist within about 2 Mpc around the source, followed by a sharp decrease to levels below 0.1 nG along the line of sight. Sources in such clusters could be active galaxies (AGNs) whose hot spots, for example, have been suggested to accelerate UHECRs [2].

Figure 3 demonstrates the influence of the cluster EGMF on the fluxes of secondary γ-rays. Note that all fluxes scale with η. This implies that for magnetized galaxy clusters and relatively soft injection spectrum $\propto E^{-2.7}$, the TeV γ-ray signal should be visible at least with HESS 2, provided $\eta \gtrsim 0.01$, whereas detectability by MAGIC and GLAST requires $\eta \gtrsim 0.2$. For harder injection spectra $\propto E^{-2.3}$ these numbers are $\eta \gtrsim 0.05$ and $\eta \gtrsim 0.4$, respectively. These figures are for a source at $d = 20$ Mpc, but depend only moderately on d.

Currently the isotropy of UHECRs at 10^{19} eV imposes only loose bounds on η due to the small statistics. Upcoming generation experiments like Auger will constrain η much better in a near future.

In Fig. 3 the one-dimensional simulation neglected proton deflection and used the 3d profile of the magnetic field projected onto the line of sight. The results demonstrate that the γ-ray fluxes below $\sim$100 TeV can be enhanced considerably by magnetic fields surrounding the source and that it is crucial to take into account the 3-dimensional nature of the problem. In the one-dimensional approximation, the path length is fixed and given by the source distance. As a result, for moderate source distances, energy loss due to pair production is negligible, and most of the energy going into photons is due to pion production whose energy loss length above $\simeq 6 \times 10^{19}$ eV is comparable or smaller than the source distance. Only the energetically subdominant low energy photon tail is influenced by magnetic fields via synchrotron emission of the pairs produced by the protons. In contrast, if 3-dimensional nucleon trajectories are taken into account, their path length can increase enormously due to deflection and confinement, especially at energies below $\sim 10^{19}$ eV where energy loss is slow and dominated by pair production. As a consequence, for steep injection spectra, the energy going into the EM channel can become dominated by pair production.

Electrons of energy E_e in a magnetic field B emit synchrotron photons of typical energy

$$E_{\rm syn} \simeq 6.8 \times 10^{11} \left(\frac{E_e}{10^{19}\ {\rm eV}}\right)^2 \left(\frac{B}{0.1\ \mu{\rm G}}\right) {\rm eV}. \tag{7}$$

The typical energy of electrons and photons produced in pion production is $\sim 5 \times 10^{18}$ eV [6]. Therefore, in a

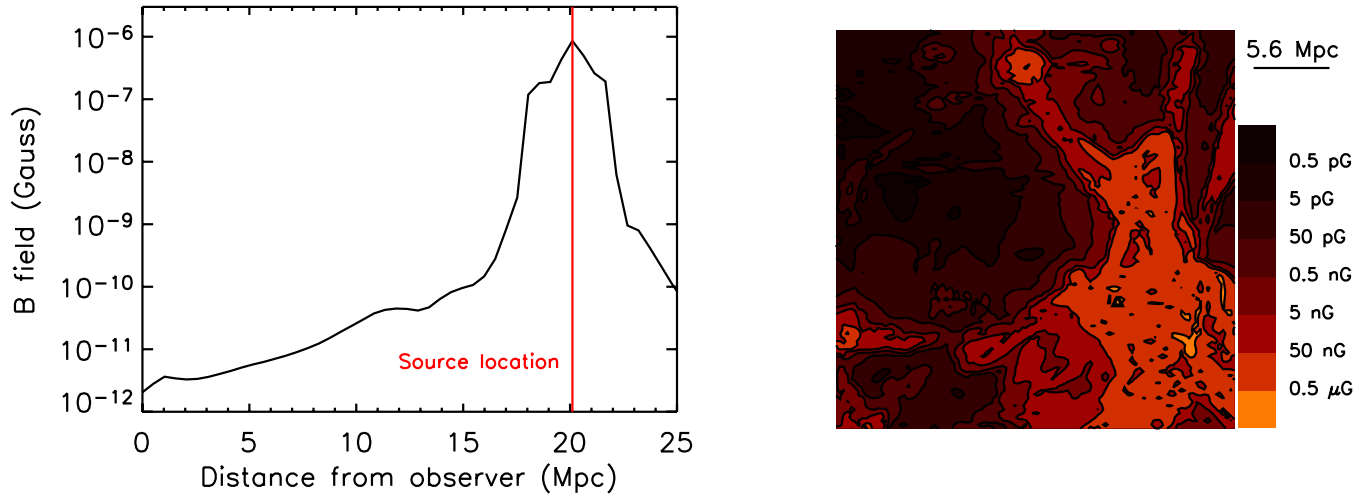

FIG. 2 (color online). Left panel: Profile of the magnetic field amplitude along the line of sight from the observer to the source for a magnetized source at 20 Mpc from the observer. Right panel: Cross section of the EGMF amplitude in the plane of the source, perpendicularly to the observer line of sight. The source is represented by a black triangle.

0.1 μG field, the synchrotron emission from the electrons produced in the first stages of an EM cascade initiated by pion production occurs mainly below $\sim$0.1 TeV. In contrast, most of the pair production occurs for proton energies E between $\simeq 10^{18}$ eV and $\simeq 4 \times 10^{19}$ eV, and gives rise to an electron energy distribution $dn/dE_e \propto E_e^{-7/4}$ up to the kinematic cut-off Eq. (1). The average electron energy is

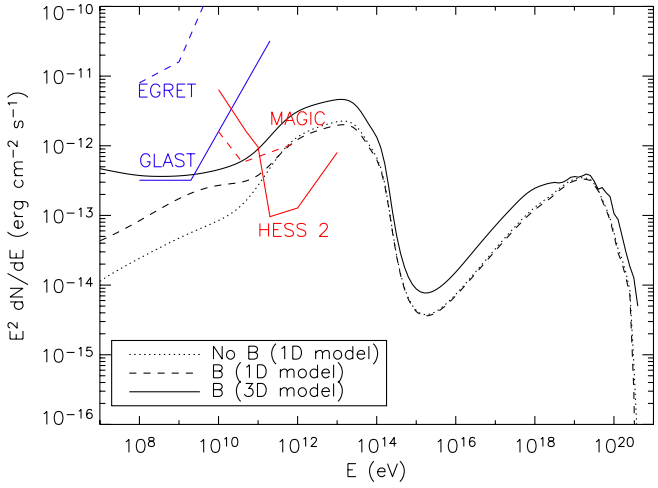

FIG. 3 (color online). Differential γ-ray fluxes (multiplied by squared energy) from photo-pion and pair production by UHECR injected with an $E^{-2.7}$ spectrum by a source at 20 Mpc. We assume the source contributes a fraction $\eta \simeq 0.2$ to the total UHECR flux, corresponding to a proton luminosity $L_{19} \simeq 4 \times 10^{42}$ erg s^{-1} in Eq. (2). Compared are different magnetic field and propagation models, as indicated: The 1D model is for the EGMF projected onto the line of sight, shown in Fig. 2, top panel, whereas the 3D model takes into account the full 3D structure, a 2D cross section of which is shown in Fig. 2, lower panel. Experimental sensitivities are as in Fig. 1.

then $\int_{E_{\rm min}}^{E_{\rm PPP}} dE_e E_e E_e^{-7/4} / \int_{E_{\rm min}}^{E_{\rm PPP}} dE_e E_e^{-7/4} \simeq 3 E_{\rm min}^{3/4} E_{\rm PPP}^{1/4}$ which is indeed much smaller than the primary proton energy E. The precise inelasticity whose energy dependence can be found in Refs. [17,24] thus depends on $E_{\rm min}$, for which kinematic expressions were given in Ref. [19]. However, we are not sensitive to the lower kinematic limit since the total energy produced $\propto \int_{E_{\rm min}}^{E_{\rm PPP}} dE_e E_e E_e^{-7/4} \simeq 4 E_{\rm PPP}^{1/4}$ is insensitive to $E_{\rm min}$ as long as $E_{\rm min} \ll E_{\rm PPP}$, but rather is dominated by the highest energies. As a consequence, the total proton energy loss rate due to pair production is dominated by the highest energy electrons close to $E_{\rm PPP}$. However, because the production cross section of these highest energy electrons is much smaller than the one for the more numerous lower energy electrons, the average inelasticity is nevertheless small, below 10^{-3} everywhere above the pair production threshold. This implies that the synchrotron spectrum from the pairs extends up to the energy given by Eq. (7) with E_e given by Eq. (1). As a result, for pair production, if the proton injection spectra are steeper than E^{-2}, most of the EM energy is produced by protons of a few times 10^{18} eV which ends up in synchrotron photons extending up to about 1 GeV, with a long tail to lower energies due to the rather flat pair spectrum. Both these effects are seen in Fig. 3.

Apart from synchrotron radiation in the magnetic fields, the pairs also produce photons via cascading in the CMB. For μGauss scale fields, the synchrotron cooling time scale of pairs of characteristic energy $E_e \sim 10^{16}$ eV, $t_{\rm synch} \simeq 40 (E_e/10^{16}\ {\rm eV})^{-1} (B/0.1\ \mu{\rm G})^{-2}$ kpc, is in fact comparable to the inverse Compton time scale in the EM cascade, $t_{\rm IC} \simeq 5 (E_e/10^{16}\ {\rm eV})$ kpc. Inverse Compton scattering dominates the photon flux above $\sim$1 TeV.

We now turn to the spatial distribution of the secondary γ-ray flux from the galaxy cluster. The magnetic fields can

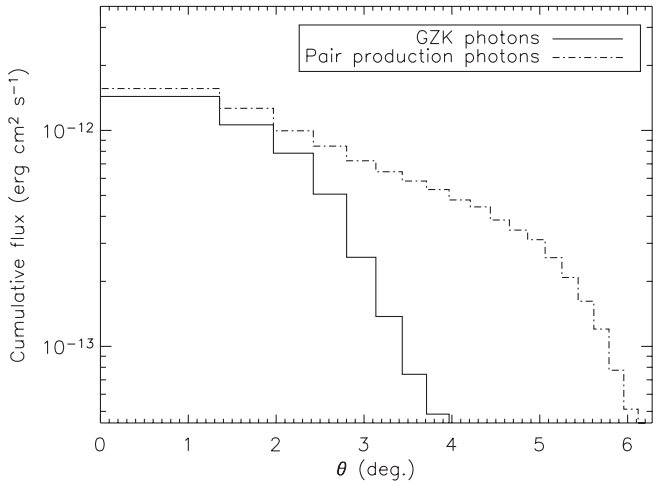

FIG. 4. Spatial extension of the counterpart in γ-ray above a TeV of the magnetized source at 20 Mpc in the 3d model of Fig. 3. The relative contributions of pair production and GZK photons are shown separately as cumulative fluxes emitted at offsets from the source center larger than θ.

lead to a GeV-TeV γ-ray halo whose structure could be observable in the case of a nearby powerful source with steep UHECR injection spectrum. In Fig. 4, the cumulative flux $\int_\theta^\infty d\Omega E^2 dN/dEd\Omega$ is represented for a source in a magnetized cluster at 20 Mpc from the observer. In this case, the γ-ray halo has two components, one due to pion production with a spatial extension of order 3°, and another, which is the dominant one, with an extension of 6°. Such a source located at 100 Mpc (like Coma) would have an extension $\sim$1°, resolvable by imaging atmospheric Čerenkov detectors.

The highest TeV photon flux in Fig. 3 can be approximated as

$$J_\gamma^{\rm ph}(E_\gamma \sim 1\ {\rm TeV}) \sim 2 \times 10^{-13} \left(\frac{\eta}{0.02}\right) {\rm cm}^{-2}\,{\rm s}^{-1}. \quad (8)$$

Requiring the TeV γ-ray flux to be dominated by the UHECR interactions rather than low energy pp interactions, $J_\gamma^{pp}(\sim{\rm TeV}) \lesssim J_\gamma^{\rm ph}(\sim{\rm TeV})$, amounts to the condition $\beta \lesssim 2.02$. As a consequence, imposing the EGRET constraint and requiring the TeV γ-ray flux to be dominated by UHECR interactions (rather than low energy pp interactions), requires a hard cosmic ray injection spectrum below ultrahigh energies.

In addition to the processes discussed above, TeV electrons accelerated at cluster shocks in galaxy clusters can also produce diffuse γ-ray emission at a comparable level through inverse Compton emission [25].

The radiation spectrum produced by pp interactions and inverse Compton scattering by shock accelerated electrons is a flat power law, $E^2 dN/dE \propto E^{2-\alpha}$ with $\alpha \sim 2$ [25]. Thus it should be distinguishable from the spectra illustrated in Fig. 3, characterized by a broken power law with $\alpha < 0$ at TeV energies. Notice that the latter is rather insensitive to the slope of the injected UHECRs as the emitting particles are produced in a cascade process.

Finally, the photon fluxes do not depend significantly on $E_{\rm max}$ in our scenarios, provided $E_{\rm max} \gtrsim$ few 10^{20} eV. They also do not depend considerably on the detailed magnetic field structure, as long as there are magnetic fields of 0.1–1 μG on scales of a few Mpc.

V. CONCLUSIONS

Ultrahigh energy cosmic rays produce secondary γ-ray from pion production and pair production on the cosmic microwave and other low energy photon backgrounds. If a significant fraction of highest energy cosmic rays is produced in galaxy clusters which are known to contain magnetic fields of fractions of a μG over Mpc length scales, the secondary γ-rays at $\sim$1 TeV energies could be detectable by γ-ray experiments such as HESS 2, and potentially also by MAGIC and GLAST at relatively lower energies. This is especially the case for relatively steep injection spectra $\propto E^{-2.6}$ above 10^{18} eV which are required by scenarios explaining the ankle by pair production of extragalactic protons. Injection spectra steeper than $\propto E^{-2.2}$, however, cannot continue down to $\sim$GeV energies. Instead, they have to become harder somewhere between GeV and ultrahigh energies to avoid over-production of photons produced in inelastic pp collisions. The advantage of the effects studied here is, however, that they do not depend on extrapolations below $\sim 10^{18}$ eV, but still lead to observable fluxes.

Our simulations have shown that the 3-dimensional structure of cosmic ray trajectories and their increased path length in μGauss scale fields around the source can considerably increase the flux and modify the spectra of photons up to $\sim$100 TeV. Pair production and pion production make comparable contributions to the γ-ray flux within a factor 2 to 3. Furthermore the γ-ray flux is expected to extend over the size of the magnetized region embedding the UHECR source, and the TeV source could therefore be spatially resolved.

In addition, γ-ray fluxes or upper limits from a given nearby extragalactic object can be used to set robust, competitive upper limits on the primary UHECR flux from this source, and thus on clustering in general.

ACKNOWLEDGMENTS

F. M. acknowledges support by the Swiss Institute of Technology through a Zwicky Prize Grant. We thank Susumu Inoue for helpful and encouraging comments.

[1] J. W. Cronin, Nucl. Phys. B, Proc. Suppl. **138**, 465 (2005).
[2] D. F. Torres and L. A. Anchordoqui, Rep. Prog. Phys. **67**, 1663 (2004).
[3] J. W. Cronin, Nucl. Phys. B, Proc. Suppl. **28**, 213 (1992); The Pierre Auger Observatory Design Report 1997 ed. 2; see also http://www.auger.org.
[4] for recent reviews see, e.g., F. Halzen and D. Hooper, Rep. Prog. Phys. **65**, 1025 (2002); A. B. McDonald, C. Spiering, S. Schonert, E. T. Kearns, and T. Kajita, Rev. Sci. Instrum. **75**, 293 (2004).
[5] for recent short reviews see, e.g., H. J. Völk, Nucl. Phys. B, Proc. Suppl. **138**, 492 (2005); astro-ph/0312585.
[6] K. Greisen, Phys. Rev. Lett. **16**, 748 (1966); G. T. Zatsepin and V. A. Kuzmin, Pis'ma Zh. Eksp. Teor. Fiz. **4**, 114 (1966) [JETP Lett. **4**, 78 (1966)].
[7] S. Gabici and F. A. Aharonian, Phys. Rev. Lett. **95**, 251102 (2005).
[8] C. Ferrigno, P. Blasi, and D. De Marco, Astropart. Phys. **23**, 211 (2005).
[9] C. Rordorf, D. Grasso, and K. Dolag, Astropart. Phys. **22**, 167 (2004).
[10] F. A. Aharonian, Mon. Not. R. Astron. Soc. **332**, 215 (2002).
[11] S. Inoue, F. A. Aharonian, and N. Sugiyama, Astrophys. J. **628**, L9 (2005).
[12] V. Berezinsky, A. Z. Gazizov, and S. I. Grigorieva, hep-ph/0204357.
[13] V. Berezinsky, A. Z. Gazizov, and S. I. Grigorieva, Phys. Lett. B **612**, 147 (2005).
[14] G. Sigl, F. Miniati, and T. A. Ensslin, Phys. Rev. D **70**, 043007 (2004).
[15] A. Mucke, R. Engel, J. P. Rachen, R. J. Protheroe, and T. Stanev, Comput. Phys. Commun. **124**, 290 (2000).
[16] G. R. Blumenthal, Phys. Rev. D **1**, 1596 (1970).
[17] M. J. Chodorowski, A. A. Zdziarski, and M. Sikora, Astrophys. J. **400**, 181 (1992).
[18] A. Mastichiadis, Mon. Not. R. Astron. Soc. **253**, 235 (1991).
[19] S. Lee, Phys. Rev. D **58**, 043004 (1998).
[20] J. R. Primack *et al.*, Astropart. Phys. **11**, 93 (1999).
[21] O. Reimer, M. Pohl, P. Sreekumar, and J. R. Mattox, Astrophys. J. **588**, 155 (2003).
[22] D. Ryu, H. Kang, and P. L. Biermann, Astron. Astrophys. **335**, 19 (1998).
[23] F. Miniati, Mon. Not. R. Astron. Soc. **337**, 199 (2002).
[24] A. Mastichiadis, R. J. Protheroe, and J. G. Kirk, Astron. Astrophys. **433**, 765 (2005).
[25] F. Miniati, Mon. Not. R. Astron. Soc. **342**, 1009 (2003).
[26] see, e.g., http://www-glast.stanford.edu.
[27] see http://www.mpi-hd.mpg.de/hfm/HESS/HESS.html.
[28] see, e.g., http://magic.mppmu.mpg.de/.